Cell Reports
Article

Cell PRESS
Open ACCESS

Molecular Identification of t^{w5}: *Vps52* Promotes Pluripotential Cell Differentiation through Cell–Cell Interactions

Michihiko Sugimoto,[1] Masayo Kondo,[1] Michiko Hirose,[2] Misao Suzuki,[4] Kazuyuki Mekada,[3] Takaya Abe,[5] Hiroshi Kiyonari,[5] Atsuo Ogura,[2] Nobuo Takagi,[6] Karen Artzt,[7] and Kuniya Abe[1,*]
[1]Technology and Development Team for Mammalian Cellular Dynamics
[2]Bioresource Engineering Division
[3]Experimental Animal Division
RIKEN BioResource Center, Tsukuba, Ibaraki 305-00074, Japan
[4]Institute of Resource Development and Analysis, Kumamoto University, Kumamoto 860-0811, Japan
[5]Laboratory for Animal Resources and Genetic Engineering, RIKEN Center for Developmental Biology, Kobe, Hyogo 650-0047, Japan
[6]Division of Bioscience, Graduate School of Environmental Earth Science, Hokkaido University, Sapporo 060-0808, Japan
[7]Insititute for Cellular and Molecular Biology, University of Texas, Austin, TX 78712, USA
*Correspondence: abe@rtc.riken.jp
http://dx.doi.org/10.1016/j.celrep.2012.10.004

SUMMARY

After implantation, pluripotent epiblasts are converted to embryonic ectoderm through cell–cell interactions that significantly change the transcriptional and epigenetic networks. An entrée to understanding this vital developmental transition is the t^{w5} mutation of the mouse *t* complex. This mutation produces highly specific defects in the embryonic ectoderm before gastrulation, leading to death of the embryonic ectoderm. Using a positional cloning approach, we have now identified the mutated gene, completing a decades-long search. The gene, *vacuolar protein sorting 52* (*Vps52*), is a mouse homolog of yeast *VPS52* that is involved in the retrograde trafficking of endosomes. Our data suggest that *Vps52* acts in extraembryonic tissues to support the growth and differentiation of embryonic ectoderm via cell–cell interactions. It is also required in the formation of embryonic structures at a later stage of development, revealing hitherto unknown functions of *Vps52* in the development of a multicellular organism.

INTRODUCTION

During an early phase of mammalian development, developmental pluripotency is maintained by a particular cell lineage. The blastocyst contains a clump of cells called the inner cell mass (ICM), surrounded by trophectoderm. The ICM consists of pluripotent cells, the epiblasts, that will contribute to the embryo proper, and primitive endodermal cells that will give rise to the extraembryonic endoderm. Remarkably, embryonic stem cells (ESCs) can be derived from the ICM. After uterine implantation, the blastocyst becomes the egg cylinder, which consists of an ectoplacental cone, extraembryonic ectoderm, visceral endoderm (VE), and embryonic ectoderm. In the egg cylinder, pluripotent epiblasts are converted to embryonic ectoderm, a columnar epithelial layer surrounding a proamniotic cavity. This morphogenetic conversion (also known as cavitation) begins at about embryonic day 5.0 (E5.0), ~1 day after implantation (Coucouvanis and Martin, 1995). Both epiblasts and embryonic ectoderm are pluripotent embryonic cells, but pluripotent cells in the blastocyst and in egg-cylinder-stage embryos display distinctly different developmental characteristics. Therefore, here we define embryonic ectoderm as the columnar epithelial cells formed after cavitation, and epiblasts as their precursors that existed before cavitation. These two cell types differ morphologically and functionally: epiblasts can be transmitted to the next generation via germline chimeras, whereas embryonic ectoderm cannot contribute to chimeras (Rossant et al., 1978). The two cell types also show qualitatively distinct epigenetic states, as exemplified by differences in their genome-wide DNA methylation patterns (i.e., low in epiblasts and higher in embryonic ectoderm; Borgel et al., 2010). Random X chromosome inactivation in female mammals is not initiated in the epiblast, but begins and is maintained stably in the embryonic ectoderm. Mouse ESCs and epiblasts within the ICM represent a ground, or naïve, state of pluripotency, whereas embryonic ectoderm and EpiSCs, stem cell lines derived from embryonic ectoderm (Brons et al., 2007; Tesar et al., 2007) correspond to a more restricted, or primed, pluripotent state, and these characteristics appear to be largely determined by growth factors in the environment (Ng and Surani, 2011).

Epiblast-embryonic ectoderm conversion is associated with significant changes in transcriptional and epigenetic networks, and cell–cell interactions between the pluripotent cells and the surrounding cells must play important roles in this transition. However, it is largely unknown which factors or genes are important for postimplantation changes. Mutants that display specific defects in the relevant processes provide an unbiased entry point for analyses. The t^{w5} mutation, which occurs in the *t* haplotype, shows highly specific defects in the embryonic ectoderm of

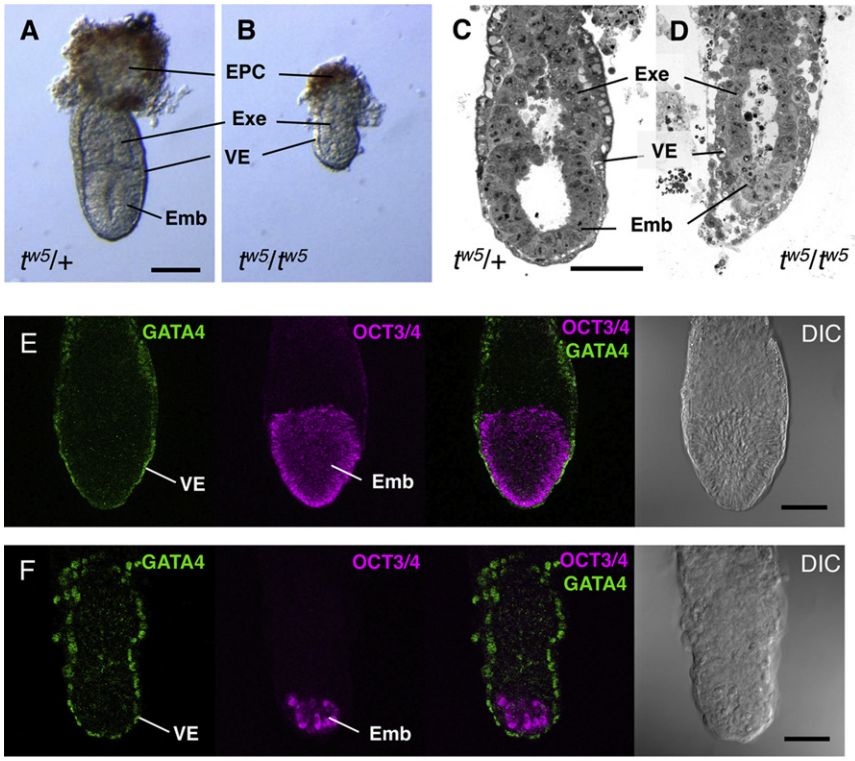

Figure 1. Growth Defects in the Embryonic Ectoderm of t^{w5}/t^{w5} Embryos

(A–D) Gross morphology (A and B) and histological sections (C and D) of $t^{w5}/+$ (A and C) and t^{w5}/t^{w5} embryos (B and D) at E6.5.

(E and F) Immunofluorescent images in $t^{w5}/+$ (E) and t^{w5}/t^{w5} embryos (F) indicate well-developed GATA4-positive VE (green) and a severe defect in OCT3/4-positive embryonic ectoderm (magenta) in the mutant. EPC, ectoplacental cone; Exe, extraembryonic ectoderm; Emb, embryonic ectoderm. Scale bars, 100 μm (A, C, and E) and 50 μm (F). VE, visceral endoderm. See also Figures S1 and S2.

pregastrulating embryos, resulting in embryonic death at approximately E6.5.

The *t* complex is a genetic region that spans ~20 cM corresponding to the proximal half of chromosome 17. The *t* haplotype is a naturally occurring variant form of the *t*-complex region that harbors four nonoverlapping inversions that cause crossover suppression between *t* haplotype and wild-type (WT) chromosomes. Thus, the *t* haplotype appears to behave genetically as if it were a single locus (Barlow, 1992; Silver, 1993; Lyon, 2005), but crossovers are observed at normal rates between two different, complementing *t* haplotypes (Silver and Artzt, 1981). Most mice with *t* haplotypes carry distinct recessive lethal mutations that critically affect important steps in embryogenesis and have been used to clarify certain features of early development (Bennett, 1975). In fact, developmental mutations located in the *t* complex are of great interest. The *T* (*Brachyury*) gene has proved to be a key player in the development of mesoderm in vertebrates (Herrmann et al., 1990), and the gene responsible for the *T*-associated maternal effect (*Tme*) turned out to be *Igf2r*, the first imprinted gene cloned in the mouse (Barlow et al., 1991). However, the causative genes identified in the *t com*plex thus far are of mutations occurring on WT chromosomes. Cloning the recessive *t*-lethals in *t* haplotypes has been a huge technical challenge. Because *t* haplotypes do not recombine with WT chromosomes, the abundant genetic reagents and resources that have been developed for analysis of WT chromosomes cannot be applied. A scarcity of polymorphic markers between complementing *t* haplotypes makes the genetic analysis of *t*-lethals even more cumbersome (Frischauf, 1985), and none of the recessive *t*-lethals that occur in the *t* haplotypes have been identified molecularly to date. A previous genetic study narrowed down the t^{w5} critical region to 750 kb (Abe et al., 2004a). In this work, we used a series of five overlapping bacterial artificial chromosome (BAC) clones to functionally rescue t^{w5} mutant embryos. We then identified a candidate gene, *vacuolar protein sorting 52* (*Vps52*), and confirmed its authenticity.

Vps52 is the mouse homolog of yeast *VPS52* that is involved in the retrograde trafficking of endosomes (Bonifacino and Rojas, 2006). Its function in the development of multicellular organisms has been totally unknown. Our data strongly suggest that via cell–cell interactions, *Vps52* acts in extraembryonic tissues, most likely in the VE, to support the developmental transition from epiblasts to embryonic ectoderm and growth, and is also required in the embryonic ectoderm lineage for embryonic vasculogenesis at a later stage of development.

RESULTS

The t^{w5}-Lethal Mutation Affects the Growth and Differentiation of Pluripotential Embryonic Cells

It is known that t^{w5} is a recessive mutation that causes death at approximately E6.5 (Bennett and Dunn, 1958). As shown in Figures 1A and 1C, WT E6.5 embryos consisted of embryonic ectoderm, VE, extraembryonic ectoderm, and an ectoplacental cone. By contrast, at the same stage, the t^{w5}/t^{w5} embryos were significantly smaller than the WT embryos (Figure 1B). Histological analysis revealed that the epithelial layer of embryonic ectoderm was not formed at all in the t^{w5}/t^{w5} embryos, whereas the extraembryonic tissues were relatively well developed (Figures 1C, 1D, and S1A–S1D). Immunofluorescence analysis with antibodies to OCT3/4, a marker for epiblast and embryonic ectoderm, and to GATA4, a VE marker, demonstrated that growth of the embryonic ectoderm was severely affected, whereas GATA4-positive VE was formed normally in t^{w5}/t^{w5} embryos (Figures 1E, 1F, and S1E–S1G).

A bromodeoxyuridine (BrdU) incorporation assay also indicated that cells in the extraembryonic tissues were actively dividing in both WT and t^{w5}/t^{w5} embryos, but the rate of cell

division was very low in the embryonic ectoderm of the mutants compared with the WT (Figure S2). These results indicate that the recessive lethal mutation in the t^{w5} haplotype affected the growth and/or differentiation of cells of the epiblast lineage before the initiation of gastrulation. Interestingly, the lethal effect was highly specific spatially, in that cavitation in the extraembryonic portion proceeded almost normally, whereas there seemed to be no evidence of cavitation in the embryonic part of the mutant embryos.

Positional Cloning of the Gene Responsible for the t^{w5} Mutation

To identify the gene responsible for t^{w5}, we used a positional cloning approach. The 750-kb critical region for the mutation (Vernet et al., 1998; Abe et al., 2004a) contains at least 42 transcription units according to the current genome databases. Genetic analysis of *t* haplotypes is technically difficult because of the scarcity of markers that distinguish different *t* haplotypes. Thus, it would be a cumbersome task to further narrow down the critical region by conventional genetic mapping. Therefore, we decided to identify t^{w5} by functional complementation through BAC transgenesis. We injected BAC clones derived from the MSM/Ms mouse (Abe et al., 2004b), an inbred strain derived from the Japanese wild mouse, *Mus musculus molossinus*, into fertilized eggs of C57BL/6 (B6) mice. Detection and measurement of the copy number and messenger RNA (mRNA) expression level of the BAC transgene (Tomida et al., 2009) were facilitated by single nucleotide polymorphisms (SNPs) that were frequently found between MSM/Ms and B6. As shown in Figure 2A, the 750-kb region was covered by five overlapping BAC clones. Eleven transgenic lines were established using those five BACs. The copy numbers of the integrated BAC transgene and the level of mRNAs transcribed from the BAC transgene in each strain were estimated by restriction fragment length polymorphism genotyping of PCR products (data not shown). The copy numbers of the integrated transgene varied from strain to strain, ranging from one to >30. For example, the copy number in the BAC5 line16 is one or two. Transcripts from the BAC transgenes were detected in all cases except for one line, which was omitted from the subsequent analysis. We also confirmed by DNA fluorescence in situ hybridization (FISH) that each BAC transgene was integrated into a single chromosomal site other than chromosome 17. For example, in BAC5 line 16, the transgene was integrated into the chromosome 1C region (Figures S3A and S3B). One or two lines of transgenic mice that carried each of the BAC constructs showing high transgene expression were selected and crossed with t^{w5} heterozygotes to make t^{w5}/+ strains carrying each BAC transgene. These were then used for functional complementation assays. After typing 497 pups, we finally ascertained that only the BAC5 transgene could rescue early embryonic lethality. Eleven pups with the t^{w5}/t^{w5};*BAC5* genotype were found among 159 offspring from the relevant cross (Table 1; Figure 2B), whereas no t^{w5}/t^{w5} homozygotes were born. Subsequent analyses of the rescued fetuses and individual pups suggested that the transgenic rescue was incomplete, because postnatal growth of the pups was affected and some of the t^{w5}/t^{w5};*BAC5* fetuses showed slight developmental retardation (Figures S3C–S3F). However, the functional rescue of embryonic lethality by the BAC5 was highly specific and reproducible, demonstrating strongly that the 177-kb BAC genomic fragment should contain the responsible gene.

BAC5 is located in one of the most gene-rich regions in the mouse genome (Abe et al., 1988) and carries at least 16 transcription units. To identify the responsible gene within this region, we cut the BAC5 insert into three pieces and repeated the rescue experiment. We found that only the 54-kb *PacI-RsrII* fragment could rescue fetuses from embryonic lethality (Figure 2A; Table 1). Finally, the 20-kb *PsiI* fragment derived from the 54-kb fragment successfully complemented the lethal phenotype (Figure 2A; Table 1). These results indicate that the responsible gene should be in this 20-kb fragment, which contains only one complete gene (*Vps52*), and just the 5′ part of the *ribosomal protein s18* (*Rps18*) gene.

In yeast, the *VPS52* gene is known to be involved in the retrograde transport of endosomes and to be a component of the Golgi-associated retrograde protein (GARP) complex (Conibear and Stevens, 2000). Up to now, however, the biological functions of *Vps52* in mouse development had not been studied.

The t^{w5} Haplotype Has a Frameshift Mutation in Exon 2 of *Vps52*

Given the results described above, it is highly likely that *Vps52* is mutated in the t^{w5} haplotype. Therefore, we sequenced the *Vps52* gene using cosmid clones isolated from the t^{w5} haplotype genomic library (Uehara et al., 1987). In exon 2 of *Vps52* of the B6 strain, there is a stretch of nine consecutive G nucleotides. However, two additional Gs were found in the stretch of the t^{w5} haplotype (Figures 2C, 2D, and S4), resulting in a frameshift mutation that generates a premature termination codon.

Because the *t* haplotype is highly diverged evolutionarily from conventional laboratory strains, a number of SNPs and indels can be found when two kinds of genome sequences are compared; therefore, the frameshift mutation may represent a *t*-haplotype-specific polymorphism that is unrelated to the t^{w5} mutant phenotype. To clarify this point, we sequenced the corresponding regions from another *t* haplotype, t^{12}, and found that this strain had nine Gs, as in the B6 strain (Figure S4).

t^{w5G} Is a Viable Revertant of the t^{w5} Haplotype that Corrects the Frameshift

t^{w5G} is an apparent spontaneous revertant that occurred 25 years ago in a mouse colony of t^{w5} tailless by tailless balanced lethal cross (D. Bennett and K. Artzt, personal communication). It showed up as a normal tailed female that, if she was a rare recombinant, should have carried a recessive outside marker, *tufted*. When she did not, the "new" *t* haplotype was rescued, established, and named t^{w5G}. This haplotype maintains all the characteristics of a complete *t* haplotype. When the *Vps52* allele from t^{w5G} was sequenced, it had 12 G nucleotides in the mutated region, restoring the frameshift with one glycine insertion (Figures 2C, 2D, and S4). These data again indicated that the frameshift mutation found is not a generic *t* haplotype change per se but is specific to the t^{w5} mutant.

As shown in Figure 2D, the predicted amino acid sequence of the t^{w5} VPS52 is the same up to glycine 33, but is followed by 36 irrelevant amino acids and then a stop. Therefore, we predicted

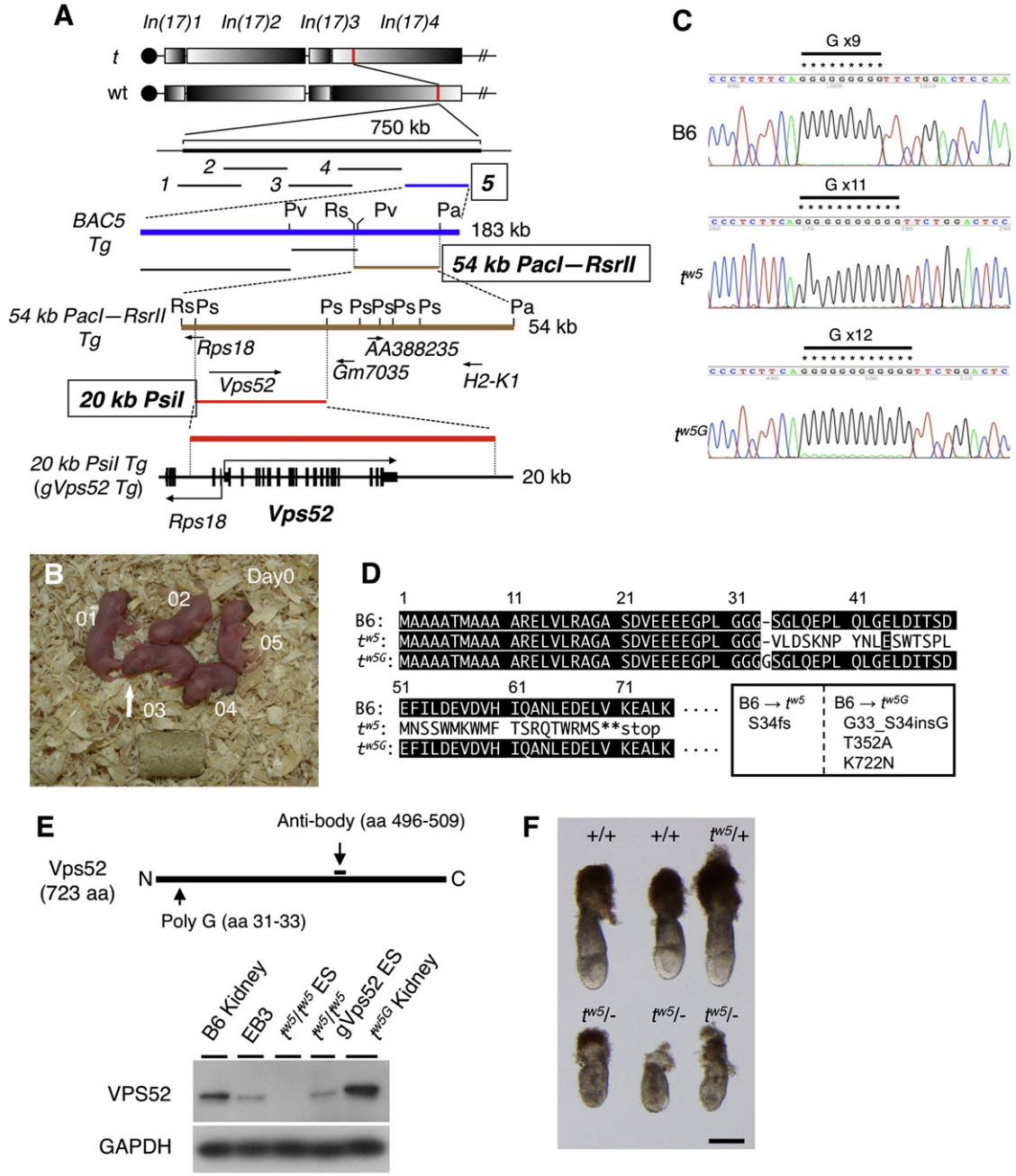

Figure 2. Identification of the Gene Responsible for the t^{w5}-Lethal Mutation

(A) Schematic diagram of our transgenic rescue experiments. *BAC5 Tg* (blue line) and DNA fragments containing the full-length genomic region of *Vps52* (brown and red lines) were able to rescue the early embryonic lethality t^{w5}.

(B) A litter of newborn mice from a t^{w5}/+;*BAC5* intercross. A rescued pup with the t^{w5}/t^{w5};*BAC5* genotype (arrow) is shown with its littermates.

(C) A frameshift mutation found in the t^{w5} haplotype. A 2 nucleotide (nt) insertion was detected at the start site of *Vps52* exon 2 compared with the B6 control strain. One more nucleotide insertion was detected in the revertant, t^{w5G} haplotype, leading to restoration of the frameshift.

(D) Estimated amino acid sequences of the VPS52 N-terminal region. The 2 nt insertions observed in the t^{w5} haplotype will cause the frameshift mutation at amino acid 34, and 3 nt insertions will result in reversion of the leading frame in the t^{w5G} haplotype.

(E) Western blot analysis with anti-VPS52 and anti-GAPDH antibodies. VPS52 was not detected in t^{w5}/t^{w5} ESCs, but was detected in both the rescued ESCs (t^{w5}/t^{w5};*gVps52*) and kidney of t^{w5G}/t^{w5G} mice.

(F) Genetic complementation test using *Vps52* knockout and t^{w5} mice. Heterozygous embryos carrying the t^{w5}/*Vps52* knockout allele (–) showed a typical lethal t^{w5}/t^{w5} phenotype, indicating that *Vps52* is the gene responsible for the t^{w5} mutation.

Scale bar, 200 μm. See also Figures S3–S5.

Table 1. Results of Transgenic Rescue Experiments

Transgenic Mouse Line	+/+	+/+;Tg	t^{w5}/+	t^{w5}/+;Tg	t^{w5}/t^{w5}	t^{w5}/t^{w5};Tg	Total
BAC1 line 8	5	8	17	35	0	0	65
BAC1 line 11	1	2	11	40	0	0	54
BAC2 line 9	8	6	7	23	0	0	44
BAC2 line 10	2	1	3	7	0	0	13
BAC3 line 4	5	16	4	35	0	0	60
BAC3 line 5	3	2	13	36	0	0	54
BAC4	0	6	13	29	0	0	48
BAC5 line 16	9	19	51	69	0	11	159
77 kb PvuI fragment line 1	1	1	9	8	0	0	19
77 kb PvuI fragment line 3	3	1	15	8	0	0	26
36 kb PvuI fragment line 1	2	2	10	22	0	0	36
36 kb PvuI fragment line 3	3	1	16	10	0	0	30
54 kb PacI-RsrII fragment	13	17	51	73	0	29	183
20 kb PsiI fragment line 1	1	2	11	22	0	7	42

that the t^{w5} allele of *Vps52* could not encode an authentic, full-length protein. To confirm this, we generated a polyclonal antibody that recognizes amino acids 496–509 of mouse VPS52 (Figure 2E), and performed a western blot analysis on lysates of B6 kidney, WT ESCs (EB3 cells), and t^{w5}/t^{w5} null ESCs (Magnuson et al., 1982). The antibody recognized a band of the expected size, 82 kDa, in the adult kidney of the B6 mice and in the WT ESCs. However, the VPS52 band was not detected in the t^{w5}/t^{w5} ESCs (Figure 2E). The ESCs transduced with the 20-kb *PsiI* genomic fragment used for the transgenic rescue experiment exhibited a band corresponding to VPS52, confirming that the t^{w5} homozygous ESCs had lost the ability to make the VPS52 protein, and that the 20-kb fragment restored the expression. Importantly, in the kidney of the revertant, t^{w5G} homozygous animal, the antibody clearly detected the VPS52 gene product, suggesting a strong correlation between the phenotypic reversion and VPS52 production (Figure 2E).

Targeted Disruption of *Vps52* Recapitulates the t^{w5} Mutant Phenotype

The results described above suggest strongly that the mutant phenotype is most likely caused by the absence of the VPS52 gene product. To test this notion, we generated a targeted mutation of the *Vps52* gene. We made a targeting vector in which *Pgk-Neo* cassettes flanked by FRT sequences (white arrowhead in Figure S5A) were positioned just upstream of exon 2. Two loxP sites were also located in introns 1 and 2 so that Cre-mediated recombination could remove exon 2 and/or the *Pgk-Neo* cassettes. We designated the targeted allele as 2lox2frt (*Neo*). We introduced the vector into ESCs and obtained three different lines with the correctly targeted mutation. All three were transmitted in the germline, and knockout mouse lines were successfully established (Figure S5B). Because these three mouse lines showed essentially the same phenotypes, only the results of line 95 are shown. Mice carrying the targeted allele showed a recessive t^{w5}-like lethal phenotype, indicating that insertion of the *Pgk-Neo* cassette into the intron 1 affected VPS52 expression, leading to death. By mating the $Vps52^{Neo}$/+ line with a *CAG-FLPe* transgenic line ubiquitously expressing the Flippase (FLP) enzyme (Kanki et al., 2006), we generated a 2lox1frt (*flox*) allele (Figures S5A, S5C, and S5D). Mice homozygous for the *flox* allele developed and grew normally, and showed normal fertility as expected. When mated with a general deleter strain, *CAG-Cre* (Matsumura et al., 2004), the *Pgk-Neo* cassette and exon 2 were removed efficiently from the $Vps52^{Neo}$/+ mice, generating a 1lox (–) allele (Figures S5A, S5C, and S5D). Although these $Vps52^{+/-}$ heterozygotes showed a completely normal phenotype, $Vps52^{-/-}$ homozygotes exhibited an early embryonic lethal phenotype similar to that found in the t^{w5}/t^{w5} embryos (data not shown). We next crossed the $Vps52^{-}$/+ heterozygotes with t^{w5}/+ mice to perform a genetic complementation test. All of the compound heterozygotes ($t^{w5}/Vps52^{-}$) isolated at E6.5 showed defects in the embryonic ectoderm typical of t^{w5}/t^{w5} embryos (Figure 2F). Based on the results of the complementation test, we conclude that *Vps52* must be the gene responsible for the t^{w5} mutation.

Vps52 Is Expressed Predominantly in the VE of Early Postimplantation Embryos

According to publicly available microarray data from the UCSC Genome Browser (http://genome.ucsc.edu/), *Vps52* is ubiquitously expressed in adult mice; however, the expression pattern of *Vps52* in embryos has not been reported. To understand its functional role in embryogenesis, we carried out in situ hybridization experiments. At E8.5, *Vps52* appeared to be highly expressed in mesenchymal tissues, but it was barely detectable in neuroepithelium of the neural tube (Figures 3A and 3B). Interestingly, extraembryonic mesodermal cells comprising the yolk sac also showed high expression. At E7.5, *Vps52* was expressed in embryonic and extraembryonic mesoderm but was barely detectable in embryonic ectoderm (Figures 3C and 3D). Because the embryonic lethal phenotype is evident at E5.5–E6.5, we examined *Vps52* expression in embryos of these stages, but failed to detect specific expression using the same probe and experimental conditions, suggesting that it has lower expression level at these stages (data not shown). Because the antibody

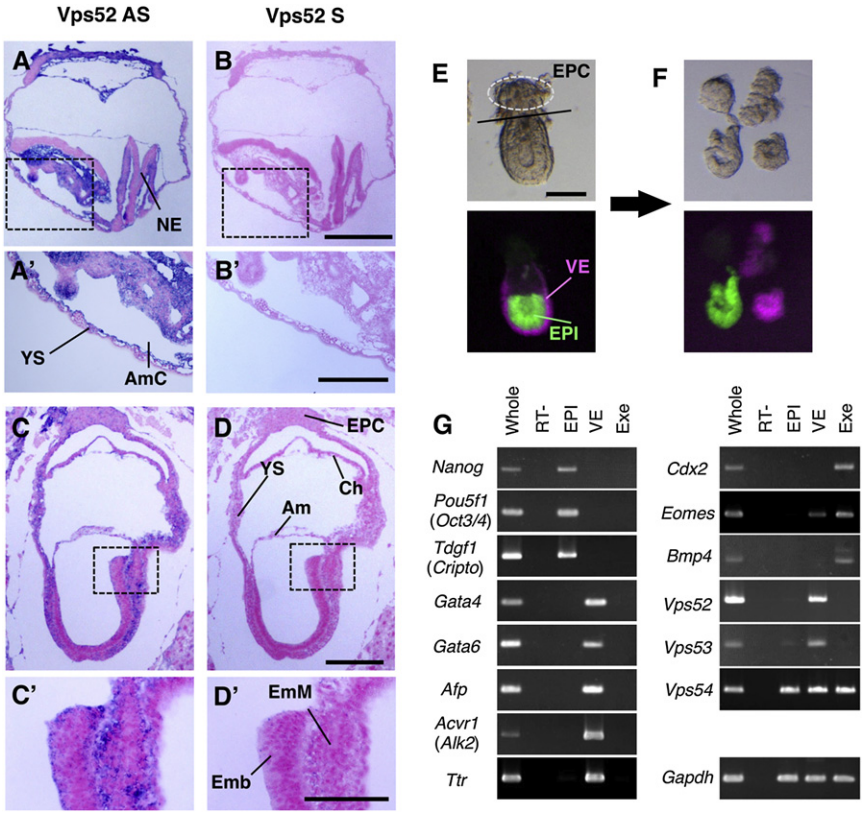

Figure 3. Expression of *Vps52* during Early Embryogenesis

(A–D) In situ hybridization analysis of E8.5 (A and B) and E7.5 embryos (C and D). *Vps52* was highly expressed in mesodermal cells. NE, neuroectoderm; YS, yolk sac; AmC, amniotic cavity; EPC, ectoplacental cone; Am, amnion; Ch, chorion; Emb, embryonic ectoderm; EmM, embryonic mesoderm.

(E and F) Separation of three embryonic tissues for tissue-specific RT-PCR analysis. *Oct4-ΔPE-EGFP* (green) and *Blimp1-mRFP* (magenta) doubly positive E5.5 embryos shown in (E) were treated enzymatically and the embryonic tissues were separated (F). EPC, ectoplacental cone; EPI, epiblast.

(G) RT-PCR analyses of *Vps52, Vps53*, and *Vps*54 genes, and tissue-specific markers. EPI, epiblast; Exe, extraembryonic ectoderm.

Scale bars, 400 μm (B), 200 μm (D and B′), and 100 μm (D′). See also Figure S6.

used for the western blot analysis was not suitable for immunohistochemistry, we tried to detect *Vps52* transcripts in early postimplantation embryos by tissue-specific RT-PCR analysis. For this analysis, we used the transgenic mouse lines *Oct4-ΔPE-EGFP* (Ohbo et al., 2003) and *Blimp1-mRFP* (Sugimoto and Abe, 2007), in which embryonic ectoderm and VE of E5.5 embryos are marked specifically by enhanced green fluorescent protein (EGFP) and monomeric red fluorescent protein (mRFP) expression, respectively (Figures 3E and S6). After removing the ectoplacental cone and enzymatic treatment, we physically separated three embryonic tissues: mRFP-positive VE, EGFP-positive embryonic ectoderm, and fluorescence-negative extraembryonic ectoderm (Figure 3F). We ensured the specificity of tissue separation by examining the expression of the fluorescence reporters in these tissue fragments (Figures 3F and S6). Using these tissue fragments, we generated complementary DNAs (cDNAs) and analyzed the expression of a series of marker genes by RT-PCR. The specific expression of various lineage markers further validated the specificity of the cDNAs. Strong expression of *Vps52* was detected in VE, whereas *Vps52* expression was barely detectable in embryonic ectoderm and extraembryonic ectoderm (Figure 3G). *Vps53*, one of the other components of the GARP complex, was also highly expressed in VE, but much weaker expression was detected in embryonic ectoderm and extraembryonic ectoderm, as in the case of *Vps52*. However, *Vps54*, another component of the GARP complex, was equally expressed in the three different embryonic tissues. This may mean that the components of GARP (*Vps52*, *Vps53*, and *Vps54*) are not necessarily coexpressed in the same cells or tissues of mouse embryos at this stage.

VPS52 Activity in Extraembryonic Tissues Is Essential for Development of the Embryo Proper

The results described above show clearly that *Vps52* was more highly expressed in VE than in embryonic ectoderm. This is counterintuitive because the developmental defects of t^{w5} embryos are manifested in the epiblasts/embryonic ectoderm but not in extraembryonic tissues. To clarify this point, we carried out epiblast lineage-specific disruption of the *Vps52* gene by crossing *Vps52*$^{flox/flox}$ female mice with *Vps52*$^{+/-}$;*Sox2-Cre* transgenic male mice. It was previously shown that the *Sox2-Cre* transgene is expressed specifically in the epiblast lineage when it is paternally transmitted (Hayashi et al., 2002, 2003).

Stage E9.5 embryos with a *Vps52*$^{flox/-}$ genotype developed normally without showing any visible defects, as these are equivalent to the t^{w5}/+ genotype (Figure 4A). Remarkably, all of the epiblast lineage-specific knockout embryos developed at least until E9.5 (Figure 4B). Although the anterior half of the embryos formed almost normally and a beating heart was observed, the development of caudal structures was clearly retarded. These morphological abnormalities were quite similar to those found in the E9.5 t^{w5}/t^{w5} embryos rescued by tetraploid complementation (Figures 4A, 4B, and S7; Sugimoto et al., 2003). At E8.5, morphological differences were not discerned between the embryo proper carrying either *Vps52*$^{flox/-}$ or *Vps52*$^{flox/-}$;*Sox2-Cre*. However, close inspection of the yolk sacs revealed blood congestion only in the *Vps52*$^{flox/-}$;*Sox2-Cre* embryos, indicating a perturbation of vascular development (Figures 4C–4F). Immunostaining with an endothelial marker, PECAM-1, demonstrated unambiguously that coordinated vasculogenesis was compromised in the epiblast lineage-specific null mutants for *Vps52* (Figures 4G and 4H), probably causing the death of these

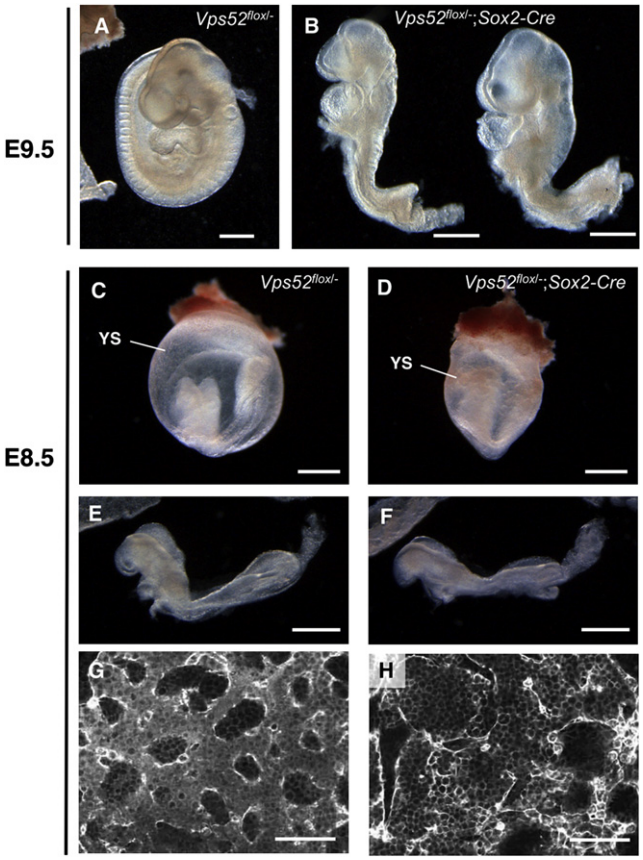

Figure 4. Epiblast Lineage-Specific Disruption of *Vps52*

(A and B) E9.5 embryos obtained from mating of $Vps52^{flox/flox}$ × $Vps52^{+/-}$;*Sox2-Cre* mice. Compared with a normal littermate (A), the epiblast lineage-specific *Vps52* knockout embryos (B) showed characteristic defects in the posterior region.

(C–H) E8.5 embryos obtained from mating of $Vps52^{flox/flox}$ × $Vps52^{+/-}$;*Sox2-Cre* mice.

(C and D) Blood congestion in the yolk sac was observed in the epiblast-specific knockout (D) but not in heterozygotes of littermates (C).

(E and F) Morphologies of the E8.5 embryo proper: $Vps52^{flox/-}$ (E) and $Vps52^{+/-}$;*Sox2-Cre* (F).

(G and H) Abnormality in yolk sac vasculogenesis in the $Vps52^{+/-}$;*Sox2-Cre* embryo. A part of the yolk sac was stained with anti-PECAM-1 antibody (white) in $Vps52^{flox/-}$ (G) and $Vps52^{+/-}$;*Sox2-Cre* (H). A normal vascular patterning was observed in the yolk sacs of normal littermates (G) but was severely disrupted in the epiblast lineage-specific knockout embryos (H). YS, yolk sac.

Scale bars, 0.5 mm (A–F) and 100 μm (G and H). See also Figure S7.

embryos. As described above, *Vps52* is highly expressed in the extraembryonic mesodermal component of the yolk sac. It is thus likely that the defects in the yolk sac shown here were caused by the absence of its expression, indicating that *Vps52* has multiple functional roles in the development of early postimplantation and midgestation-stage embryos.

Vps52 Expression in VE Promotes Pluripotential Cell Differentiation through Cell–Cell Interactions

Pluripotent ESC lines have been successfully isolated from t^{w5}/t^{w5} blastocysts (Magnuson et al., 1982). To establish a model system to study developmental defects of the t^{w5}, we used this line to make embryoid bodies (EBs) in vitro. The ESCs formed EBs composed of undifferentiated cell aggregates surrounded by a layer of GATA4-positive, primitive endoderm-like cells. However, the t^{w5}/t^{w5} EBs could not differentiate further and appeared to be arrested at the same developmental stage (Figures 5A, 5C, and 5D), whereas the WT EBs initiated cavitation and developed into cystic EBs. This suggests that a transition from simple EBs to more developed EBs is somehow blocked in the t^{w5}/t^{w5} ESCs, reminiscent of the t^{w5}/t^{w5} homozygotes. We transduced the ESCs with the 20-kb *PsiI* fragment containing *Vps52* (Figure 2A). Most of the EBs generated from the transduced ESCs (t^{w5}/t^{w5};*gVps52*) formed cystic structures in which pulsation of myocardial cells was frequently observed (Figures 5B, 5E, and 5F). This suggests that *Vps52* expression might promote t^{w5}/t^{w5} ESCs from a developmentally inert state to a cellular state poised for further differentiation. Restoration of developmental potential was also achieved by a *Vps52* cDNA construct. As shown in Figure 5G, full-length cDNA driven by a native *Vps52* promoter was introduced into the t^{w5}/t^{w5} ESCs. The resultant ESCs, t^{w5}/t^{w5};*cVps52*, developed to cystic EBs efficiently.

A chimeric EB formation assay was carried out to test whether VPS52 is involved in cell–cell interactions that promote the differentiation of ESCs. The t^{w5}/t^{w5} ESCs were first labeled with an RFP, tdTomato (t^{w5}/t^{w5};*tdTomato*; Figure 6A), and then mixed with t^{w5}/t^{w5};*gVps52* ESCs (Figure 5B) at a ratio of 3:1. Then the mixture was induced to form EBs. After 3 days of induction, several EBs exhibited structures similar to postimplantation embryos, with a cavity surrounded by an epithelial layer of embryonic ectoderm (Figure 6B). The epithelial layer was surrounded by a layer of endoderm-like cells (indicated by arrows in Figure 6B). Remarkably, the outer layer was devoid of red fluorescence, indicating that they were derived from the t^{w5}/t^{w5};*gVps52* cells, whereas the internal ectoderm was mostly t^{w5}/t^{w5};*tdTomato* cells. These EBs eventually developed to cystic EBs at day 7 of differentiation (Figure 6C). These results suggest that cells expressing *Vps52* contribute efficiently and preferentially to VE, which in turn induces cavitation of the t^{w5}/t^{w5} ESCs. However, in contrast to studies using mouse embryos, in which the involvement of extraembryonic ectoderm cannot be ruled out, this ESC study suggests that the expression of *Vps52* only in the endoderm—probably VE—was sufficient to induce differentiation of the t^{w5}/t^{w5} ESCs, which would otherwise be arrested as simple EBs. Thus, VPS52 is clearly a key factor in the proper function of VE. Our data confirm that it triggers a series of developmental events in early postimplantation embryos through cell–cell interactions (Figure 7A).

DISCUSSION

Sixteen complementation groups that cause embryonic death at specific developmental stages have been defined in *t* haplotypes. Up to now, however, no gene that is responsible for any classic *t*-lethal recessive mutation had been identified. Here, we have unambiguously demonstrated that *Vps52* is the gene responsible for t^{w5}, one of the classic, early-acting *t*-lethals.

More than 60 *VPS* genes have been identified in budding yeast as being involved in the sorting of acid hydrolases to the vacuole

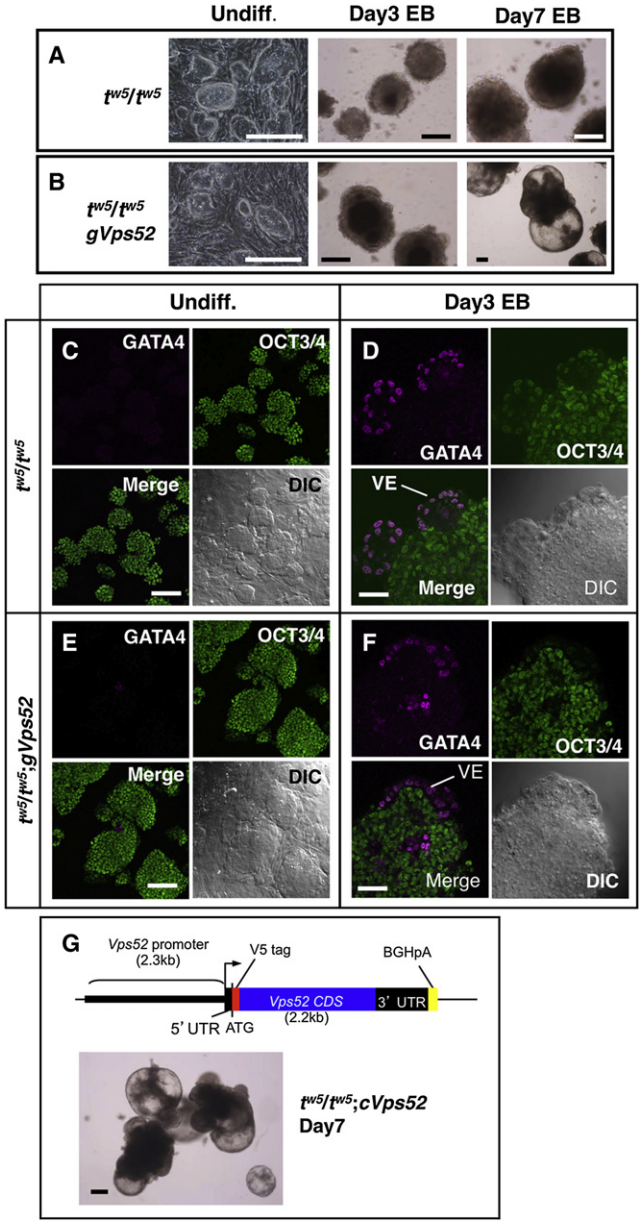

Figure 5. Phenotypic Rescue of t^{w5}/t^{w5} ESCs with the *Vps52* Transgene

(A and B) Complementation of the t^{w5}/t^{w5} ESC defect with the *Vps52* transgene. t^{w5}/t^{w5} ESCs can barely differentiate into cystic EBs (A), whereas introduction of the *Vps52* genomic fragment (t^{w5}/t^{w5};*gVps52*) leads to efficient differentiation of cystic EBs (B).

(C–F) Expression of the VE marker (GATA4) and the epiblast/embryonic ectoderm marker (OCT3/4). In undifferentiated cells, GATA4 (magenta) staining was essentially negative for undifferentiated t^{w5}/t^{w5} ESCs (C) and t^{w5}/t^{w5};*gVps52* ESCs (E), whereas OCT3/4 (green) showed positive immunostaining for both cell lines. GATA4-positive VE appeared to form in the aggregates of t^{w5}/t^{w5} ESCs (D) and t^{w5}/t^{w5};*gVps52* ESCs (F).

(G) Rescue of the differentiation defect of t^{w5}/t^{w5} EBs by introduction of *Vps52* cDNA. In the rescue experiments ([A], [B], and Figure 2A), the 20-kb *Vps52* genomic fragment was used. The same rescue effect was obtained by using *Vps52* cDNA alone driven by the endogenous *Vps52* promoter.

Scale bars, 200 μm (A, B, and G), and 100 μm (C–F).

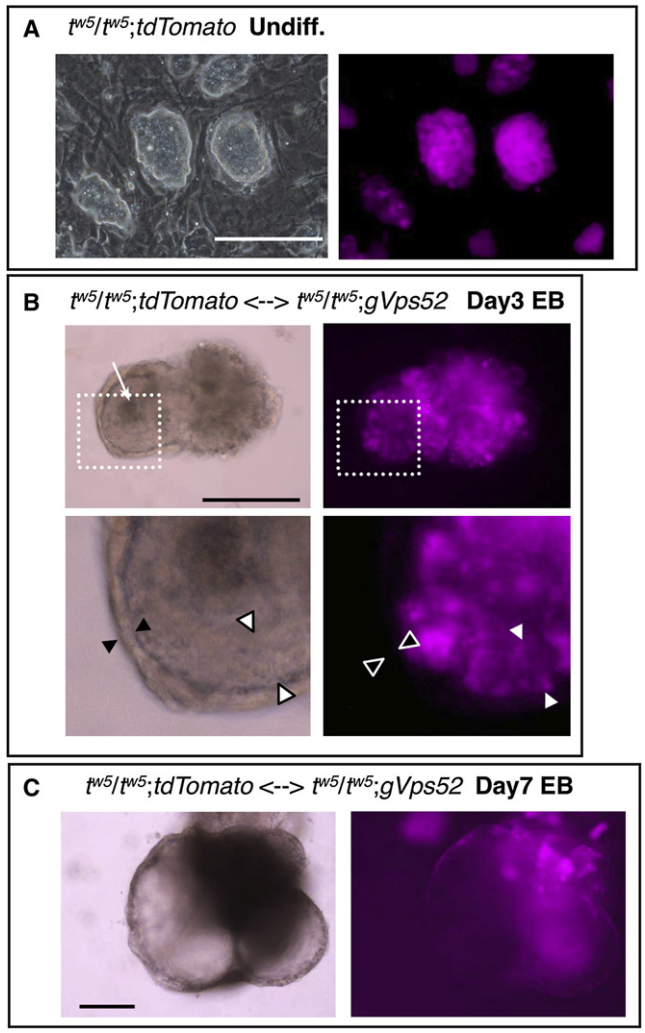

Figure 6. Chimeric EB Assay Reveals that *Vps52* Expression in VE Promoted the Differentiation of Embryonic Ectoderm via Cell–Cell Interactions

(A) A t^{w5}/t^{w5} ESC line constitutively expressing the RFP tdTomato (magenta).

(B) Chimeric EB formed after 3 days of differentiation (day 3 EB). t^{w5}/t^{w5};*tdTomato* ESCs (A) were mixed with t^{w5}/t^{w5};*gVps52* ESCs (Figure 5B) at a ratio of 3:1, and EB formation was observed. A cavity inside the EB is indicated by a white arrow. VE-like cells (marked with black arrowheads) did not express tdTomato, indicating that they had the t^{w5}/t^{w5};*gVps52* genotype. Inner cells surrounded by the VE-like cells showed tdTomato expression and appeared to form an epithelial layer of embryonic ectoderm (marked with white arrowheads).

(C) The chimeric t^{w5}/t^{w5};*tdTomato* ↔ t^{w5}/t^{w5};*gVps52* EB was able to develop to a fully expanded, cystic EB.

Scale bars, 200 μm.

(Bowers and Stevens, 2005). *VPS52* is one of the core components of the GARP complex that is required for retrograde transport from early and late endosomes to the late Golgi in yeast cells (Conibear and Stevens, 2000). The components of the complex (*VPS52*, *VPS53*, and *VPS54*) have been found in organisms ranging from yeasts to humans (Bonifacino and Rojas, 2006). Recently, the mammalian ortholog of the fourth component,

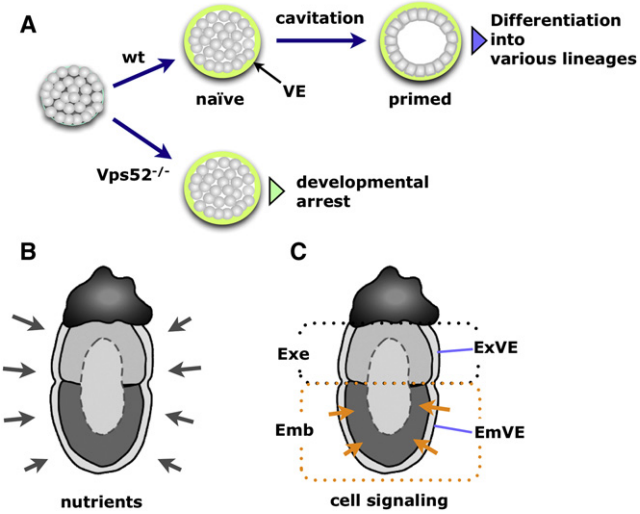

Figure 7. Model for the Function of *Vps52* in the Differentiation of Pluripotent Cells

(A) VE cells (green) emerge from an aggregate of naive pluripotent cells and form a layer of cells surrounding the pluripotent cells. This differentiation step may not need the function of VPS52. However, VPS52 expression in the VE is required for transition from the naive to the primed state.

(B) VPS52 is involved in nutrient uptake through VE.

(C) VPS52 is involved in cell signaling between embryonic visceral endoderm (EmVE) cells and epiblast/embryonic ectoderm, leading to the growth and differentiation of naive pluripotent cells. Exe, extraembryonic part of the egg cylinder; Emb, embryonic part of the egg cylinder; ExVE, extraembryonic visceral endoderm.

Vps51, was identified as being Ang2/fat-free (Pérez-Victoria et al., 2010). The primary role of the GARP complex is in the reception of endosome-derived transport carriers at the trans-Golgi network (Pérez-Victoria et al., 2008). However, the effect of GARP-disrupting mutations on development extends to a broad range of cellular functions (Bonifacino and Hierro, 2011).

It is known that in yeast cells, the loss of each component of the GARP complex causes identical phenotypes with reduced growth rates. In mice, the *wobbler* mutant, which exhibits motor neuron degeneration as well as defects in spermatid formation, harbors a missense mutation in the C-terminal region of *Vps54* (Schmitt-John et al., 2005). The *wobbler* seems to be a hypomorph of *Vps54*, because homozygotes carrying a gene trap null allele die between E11.5 and E12.5, presumably from cardiovascular malfunction (Schmitt-John et al., 2005). Mutations in either *Vps52* or *Vps53,* the other components of GARP, have not been reported in mice. Our data show that *Vps52* exhibits cell type-specific and tissue-specific functions, and that *Vps52* has multiple developmental roles during mammalian embryogenesis. Moreover, these phenotypes of *Vps52* mutants are quite different from those of *Vps54* mutants, implying that *Vps52* and *Vps54* play distinct roles in mammalian development depending on the cell types in which they are expressed. Finally, our embryonic tissue-specific RT-PCR analysis showed that *Vps52* was predominantly expressed only in the VE, whereas *Vps54* was expressed in all three tissues examined. Thus, *Vps52* and *Vps54* may not act at the same time in the GARP complex at this developmental stage.

The VE is an extraembryonic cell layer that performs critical functions during embryogenesis (Bielinska et al., 1999). The traditional role attributed to the VE involves nutrient uptake and transport (Figure 7B), and in a previous study (Sugimoto et al., 2003), t^{w5}/t^{w5} embryos exhibited defects in endocytosis, with a great reduction in uptake of horseradish peroxidase from the incubation medium. Endocytic defects in the t^{w5}/t^{w5} embryos were apparent in the entire VE, but reduced cell proliferation was seen specifically in the embryonic ectoderm/epiblast. Therefore, low endocytic activity of the VE alone may not account for the severe phenotype found in the embryonic ectoderm.

Another possibility is that *Vps52* is involved in the cell-signaling function of VE, which is known to be a signaling center required for development and patterning. During the cavitation process, a reciprocal interaction between VE and epiblast occurs, and involvement of BMP family members has been proposed (Coucouvanis and Martin, 1995, 1999). We found that *Vps52*-expressing t^{w5}/t^{w5} ESCs formed the outer endodermal layer of EBs to induce cavitation in otherwise cavitation-defective t^{w5}/t^{w5} ESCs. The mutant phenotypes of BMP-related genes and transforming growth factor β (TGF-β) superfamily genes resemble those of the t^{w5}/*Vps52* mutant in several aspects (Bielinska et al., 1999). Furthermore, some of those signaling factors showed restricted expression in the VE associated with the embryonic ectoderm (EmVE), whereas relatively few signaling factors displayed predominant expression in extraembryonic VE (ExVE; Pfister et al., 2007). Collectively, these results suggest that specific abnormalities in the embryonic part of the t^{w5} mutant may be caused by defects in cell signaling between the EmVE and embryonic ectoderm (Figure 7C). In addition, analyses of other mutations in genes involved in retrograde transport, such as *Hb58*/*Vps26* (Radice et al., 1991; Lee et al., 1992) and *Snx1*/*Snx2* (Schwarz et al., 2002; Griffin et al., 2005), indicate that these genes also act in the VE-derived tissues to support growth of the embryo proper. Even though the t^{w5}/*Vps52* mutant exhibited a phenotypic resemblance to known signaling mutants and/or the *Vps* mutants, it still showed more severe dysfunctions than did any of these mutants. Given that endocytosis appears to be involved in the regulation of most of the major developmental signaling pathways (Seto et al., 2002; Sorkin and von Zastrow, 2009), it is tempting to speculate that *Vps52* acts as a key player in orchestrating multiple signaling pathways that operate through the endocytic machinery during early mammalian development.

We were able to reconstitute defects of t^{w5} null embryos using the EB differentiation system (Figures 5 and 6), which should enable progress in future biochemical/proteomic studies. Expression of the *Vps52* transgene rescued the differentiation defect in t^{w5} null cells arrested in a naïve pluripotent state. The developmental transition from a naive to a primed state of pluripotent cells (or vice versa) is currently under intense investigation, and this process is thought to be greatly influenced by signaling factors (Ng and Surani, 2011). It should be possible to facilitate this conversion process through the manipulation of *Vps52* activity.

In summary, we have identified *Vps52* as being responsible for the t^{w5} mutation, and revealed development-specific functions

of this gene, which was formerly thought to be solely involved in retrograde endocytic transport. This provides an entrée into the functional study of *Vps52* and related molecules, and the interrelations between endocytic machinery and developmental cell signaling in mammalian embryos.

EXPERIMENTAL PROCEDURES

Mice

The mouse strains t^{w5} (RBRC01202), t^{w5G} (RBRC01203), *CAG-FLPe* (RBRC01834; Kanki et al., 2006), *CAG-Cre* (RBRC01828; Matsumura et al., 2004), *Blimp1-mRFP* (RBRC01830; Sugimoto and Abe, 2007), and *Oct4-ΔPE-EGFP* (RBRC00821; Ohbo et al., 2003) were provided by the Experimental Animal Division of the RIKEN BioResource Center (BRC), through the National Bio-Resource Project of MEXT, Japan. The t^{w5} mice were backcrossed more than five times to C57BL/6 (B6) mice before they were used. *Sox2-Cre* mice (stock no. 004783; Hayashi et al., 2002) were purchased from the Jackson Laboratory (Bar Harbor, ME). All methods were approved by the Institutional Animal Experiment Committee of RIKEN Tsukuba Institute.

Generation of Transgenic Mice for Genetic Rescue Experiments

Five BAC clones derived from the Japanese wild mouse strain MSM/Ms were used to generate BAC transgenic mice (Abe et al., 2004b). The BAC clones are available from the DNA Bank of RIKEN BRC (http://dna.brc.riken.jp/index.html). Four subfragments of the BAC5 clone were also used to produce transgenic mice for subsequent rescue experiments. The mice generated in this study have been deposited at the Experimental Animal Division, RIKEN BRC.

Generation of Conditional Knockout Mice

The *Vps52* conditional knockout mice (accession number CDB0767K; http://cdb.riken.jp/arg/mutant%20mice%20list.html) were generated essentially as described previously (http://www.cdb.riken.jp/arg/Methods.html). A targeting vector in which exon 2 of *Vps52* is flanked by two *loxP* sites with an *FRT-Pgk-Neo-FRT* sequence (Figure S5) was introduced into TT2 ESCs (Yagi et al., 1993). Three independent candidate ESC lines were obtained, and successful homologous recombination was confirmed by southern blotting and PCR. All three lines contributed to germline chimeras, from which $Vps52^{+/Neo}$ mutant mice were obtained. The $Vps52^{+/Neo}$ and *CAG-FLPe* strains were crossed to produce $Vps52^{+/flox}$ mice. The following primer set was used for genotyping: (1) GGGATCACCTGGAATAGCTG, (2) GCCAGAGGCCACTTG TGTAG, (3) GGGCTTGGATCTGAAACATC, and (4) GTGCCGGAGTAAGTGG GTC (see Figure S5).

Immunofluorescence

Whole-mount immunofluorescence analysis was done as previously described (Sugimoto and Abe, 2007). Fluorescent images were captured with an LSM 510 META laser scanning microscope (Carl Zeiss, Oberkochen, Germany). The primary antibodies were OCT3/4 (1:300, sc-8628; Santa Cruz Biotechnology, Santa Cruz, CA), GATA4 (1:300, sc-9053; Santa Cruz Biotechnology), and PECAM1 (1:25, 550274; BD Biosciences, San Jose, CA). The secondary antibodies were anti-goat immunoglobulin G (IgG) Alexa Fluor 594 (1:500, A11058; Life Technologies), anti-rabbit IgG Alexa Fluor 488 (1:500, A11058; Life Technologies), and anti-rat IgG Alexa Fluor 594 (1:500, A11007; Life Technologies).

Western Blotting

A rabbit anti-VPS52 antibody was raised against a synthetic peptide corresponding to VPS52 amino acids 496–509 (PQRLGGLDTRPHYI), followed by affinity purification (Sigma-Aldrich Japan, Tokyo, Japan). Membrane was reacted with anti-VPS52 (1:1000) and anti-GAPDH (1:10,000, sc-32233; Santa Cruz Biotechnology) antibodies. Signals were detected with an ECL Plus Western Blotting Detection Kit (GE Healthcare, Little Chalfont, UK).

In Situ Hybridization

A 610-bp DNA fragment corresponding to nucleotide positions 1671–2280 was amplified by PCR from a full-length *Vps52* cDNA clone (RIKEN FANTOM clone ID: D130068D18; Carninci et al., 2005), and digoxigenin-labeled sense and antisense RNA probes were prepared using the DIG RNA Labeling Mix (Roche, Basel, Switzerland). Paraffin-wax-embedded sections (6 μm) of E5.5–E8.5 mouse embryos were obtained from Genostaff Co. (Tokyo, Japan) and hybridized at 60°C for 16 hr. Specific signals were detected with a combination of alkaline phosphatase-conjugated anti-digoxigenin antibody (Roche) and NBT/BCIP (Sigma-Aldrich), followed by counterstaining with Kernechtrot Stain Solution (Muto Pure Chemicals, Tokyo, Japan).

Embryonic-Tissue-Specific RT-PCR

E5.5 embryos were collected from matings of *Oct4-ΔPE-EGFP* and *Blimp1-mRFP* mice. Separation of embryonic tissues was carried out as previously described (Nagy et al., 2003) with minor modifications. To ensure the absence of contamination of embryonic tissues, fluorescent microscopy was used to check for reporter gene expression (see Figures 3 and S6). RNA was purified with RNeasy Kits (QIAGEN, Venlo, The Netherlands) from pools of tissues isolated from 16 embryos. Reverse transcription and cDNA amplification were performed using a WT-Ovation Pico RNA Amplification System (NuGEN Technologies, San Carlos, CA). Primer sets and conditions of the PCR reactions are shown in Table S1.

Plasmids

The *Vps52* cDNA sequence amplified from full-length *Vps52* cDNA was cloned into pENTR/D-TOPO (Life Technologies). To generate a *pCMV-Vps52*, the insert was transferred into pcDNA3.1/nV5-DEST using Gateway technology (Life Technologies). To construct *pVps52-V5-Vps52*, a 2.5-kb fragment containing a promoter and the 5′ untranslated region of *Vps52* was amplified from a BAC clone (RP23-213I16) and inserted into *pCMV-Vps52*, and the CMV promoter was replaced using an In-Fusion HD Cloning Kit (Takara Bio, Shiga, Japan). To generate *pCAGGS-tdTomato*, a BamHI/HindII fragment of *pREST-B tdTomato* (Shaner et al., 2005) was cloned into a *pCAGGS* expression vector (Niwa et al., 1991) by blunt-end ligation using a DNA Blunting Kit (Takara Bio).

ESC Culture

The t^{w5}/t^{w5} ESC line (Magnuson et al., 1982) was maintained on mitomycin C-treated mouse embryonic fibroblasts in minimum essential medium α (MEMα; Sigma-Aldrich) supplemented with 14% knockout serum replacement (KSR; Life Technologies), 1% fetal bovine serum (FBS; Life Technologies), 1,000 U/ml leukemia inhibitory factor (LIF), 0.1 mM 2-mercaptoethanol, 1× nonessential amino acids, 2 mM L-glutamine. EB3 ESCs (AES0139; Niwa et al., 2002; Ogawa et al., 2004) were provided by the Cell Bank of the RIKEN BioResource Center and maintained under feeder-free conditions according to the supplied protocol. Transfection was done using Lipofectamine 2000 (Life Technologies).

SUPPLEMENTAL INFORMATION

Supplemental Information includes Extended Experimental Procedures, seven figures, and one table and can be found with this article online at http://dx.doi.org/10.1016/j.celrep.2012.10.004.

LICENSING INFORMATION

ACKNOWLEDGMENTS

We thank Misako Yuzuriha, Rieko Ikeda, and Peggy Centilli for help with experiments. We are indebted to Dr. T. Magnuson for the t^{w5}/t^{w5} ESC line. We also thank Drs. A. Toyoda and Y. Sakaki for genome sequencing, N. Mise for advice on ESC work, R. Tsien for *pREST-B tdTomato*, J. Miyazaki for the *pCAGGS* vector, Y. Mishina for valuable comments on the histological data, and

D. Schlessinger for a critical reading of the manuscript and valuable suggestions. K. Abe and K. Artzt dedicate this work to their mentor, Dorothea Bennett (1929–1990), who was the driving force behind this work and who personally recognized the significance of t^{w5G}. K. Abe dedicates this work also to Taeko Abe for her help in the early part of the t^{w5} project and her constant support. This work was supported in part by the Ministry of Education, Culture, Sports, Science and Technology of Japan (to M.S. and K. Abe).

Received: August 17, 2012
Revised: October 2, 2012
Accepted: October 5, 2012
Published: November 8, 2012

REFERENCES

Abe, K., Wei, J.F., Wei, F.S., Hsu, Y.C., Uehara, H., Artzt, K., and Bennett, D. (1988). Searching for coding sequences in the mammalian genome: the H-2K region of the mouse MHC is replete with genes expressed in embryos. EMBO J. *7*, 3441–3449.

Abe, K., Yuzuriha, M., Sugimoto, M., Ko, M.S., Brathwaite, M., Waeltz, P., and Nagaraja, R. (2004a). Gene content of the 750-kb critical region for mouse embryonic ectoderm lethal tcl-w5. Mamm. Genome *15*, 265–276.

Abe, K., Noguchi, H., Tagawa, K., Yuzuriha, M., Toyoda, A., Kojima, T., Ezawa, K., Saitou, N., Hattori, M., Sakaki, Y., et al. (2004b). Contribution of Asian mouse subspecies Mus musculus molossinus to genomic constitution of strain C57BL/6J, as defined by BAC-end sequence-SNP analysis. Genome Res. *14*, 2439–2447.

Barlow, D.P. (1992). Cloning development mutants from the mouse t complex. In Development: The Molecular Genetic Approach, V.E.A. Russon, S. Brody, D. Cove, and S. Ottolenghi, eds. (Berlin, Germany: Springer-Verlag GmbH), pp. 394–408.

Barlow, D.P., Stöger, R., Herrmann, B.G., Saito, K., and Schweifer, N. (1991). The mouse insulin-like growth factor type-2 receptor is imprinted and closely linked to the Tme locus. Nature *349*, 84–87.

Bennett, D. (1975). The T-locus of the mouse. Cell *6*, 441–454.

Bennett, D., and Dunn, L.C. (1958). Effects on embryonic development of a group of genetically similar lethal alleles derived from different populations of wild house mice. J. Morphol. *103*, 135–157.

Bielinska, M., Narita, N., and Wilson, D.B. (1999). Distinct roles for visceral endoderm during embryonic mouse development. Int. J. Dev. Biol. *43*, 183–205.

Bonifacino, J.S., and Rojas, R. (2006). Retrograde transport from endosomes to the trans-Golgi network. Nat. Rev. Mol. Cell Biol. *7*, 568–579.

Bonifacino, J.S., and Hierro, A. (2011). Transport according to GARP: receiving retrograde cargo at the trans-Golgi network. Trends Cell Biol. *21*, 159–167.

Borgel, J., Guibert, S., Li, Y., Chiba, H., Schübeler, D., Sasaki, H., Forné, T., and Weber, M. (2010). Targets and dynamics of promoter DNA methylation during early mouse development. Nat. Genet. *42*, 1093–1100.

Bowers, K., and Stevens, T.H. (2005). Protein transport from the late Golgi to the vacuole in the yeast Saccharomyces cerevisiae. Biochim. Biophys. Acta *1744*, 438–454.

Brons, I.G., Smithers, L.E., Trotter, M.W., Rugg-Gunn, P., Sun, B., Chuva de Sousa Lopes, S.M., Howlett, S.K., Clarkson, A., Ahrlund-Richter, L., Pedersen, R.A., and Vallier, L. (2007). Derivation of pluripotent epiblast stem cells from mammalian embryos. Nature *448*, 191–195.

Carninci, P., Kasukawa, T., Katayama, S., Gough, J., Frith, M.C., Maeda, N., Oyama, R., Ravasi, T., Lenhard, B., Wells, C., et al.; FANTOM Consortium; RIKEN Genome Exploration Research Group and Genome Science Group (Genome Network Project Core Group). (2005). The transcriptional landscape of the mammalian genome. Science *309*, 1559–1563.

Conibear, E., and Stevens, T.H. (2000). Vps52p, Vps53p, and Vps54p form a novel multisubunit complex required for protein sorting at the yeast late Golgi. Mol. Biol. Cell *11*, 305–323.

Coucouvanis, E., and Martin, G.R. (1995). Signals for death and survival: a two-step mechanism for cavitation in the vertebrate embryo. Cell *83*, 279–287.

Coucouvanis, E., and Martin, G.R. (1999). BMP signaling plays a role in visceral endoderm differentiation and cavitation in the early mouse embryo. Development *126*, 535–546.

Frischauf, A.M. (1985). The T/t complex of the mouse. Trends Genet. *1*, 100–103.

Griffin, C.T., Trejo, J., and Magnuson, T. (2005). Genetic evidence for a mammalian retromer complex containing sorting nexins 1 and 2. Proc. Natl. Acad. Sci. USA *102*, 15173–15177.

Hayashi, S., Lewis, P., Pevny, L., and McMahon, A.P. (2002). Efficient gene modulation in mouse epiblast using a Sox2Cre transgenic mouse strain. Mech. Dev. *119*(*Suppl 1*), S97–S101.

Hayashi, S., Tenzen, T., and McMahon, A.P. (2003). Maternal inheritance of Cre activity in a Sox2Cre deleter strain. Genesis *37*, 51–53.

Herrmann, B.G., Labeit, S., Poustka, A., King, T.R., and Lehrach, H. (1990). Cloning of the T gene required in mesoderm formation in the mouse. Nature *343*, 617–622.

Kanki, H., Suzuki, H., and Itohara, S. (2006). High-efficiency CAG-FLPe deleter mice in C57BL/6J background. Exp. Anim. *55*, 137–141.

Lee, J.J., Radice, G., Perkins, C.P., and Costantini, F. (1992). Identification and characterization of a novel, evolutionarily conserved gene disrupted by the murine H beta 58 embryonic lethal transgene insertion. Development *115*, 277–288.

Lyon, M.F. (2005). Elucidating mouse transmission ratio distortion. Nat. Genet. *37*, 924–925.

Magnuson, T., Epstein, C.J., Silver, L.M., and Martin, G.R. (1982). Pluripotent embryonic stem cell lines can be derived from tw5/tw5 blastocysts. Nature *298*, 750–753.

Matsumura, H., Hasuwa, H., Inoue, N., Ikawa, M., and Okabe, M. (2004). Lineage-specific cell disruption in living mice by Cre-mediated expression of diphtheria toxin A chain. Biochem. Biophys. Res. Commun. *321*, 275–279.

Nagy, A., Gertsenstein, M., Vintersten, K., and Behringer, R. (2003). Manipulating the Mouse Embryo: A Laboratory Manual, Third Edition (Cold Spring Harbor, N.Y.: Cold Spring Harbor Laboratory Press).

Ng, H.H., and Surani, M.A. (2011). The transcriptional and signalling networks of pluripotency. Nat. Cell Biol. *13*, 490–496.

Niwa, H., Yamamura, K., and Miyazaki, J. (1991). Efficient selection for high-expression transfectants with a novel eukaryotic vector. Gene *108*, 193–199.

Niwa, H., Masui, S., Chambers, I., Smith, A.G., and Miyazaki, J. (2002). Phenotypic complementation establishes requirements for specific POU domain and generic transactivation function of Oct-3/4 in embryonic stem cells. Mol. Cell. Biol. *22*, 1526–1536.

Ogawa, K., Matsui, H., Ohtsuka, S., and Niwa, H. (2004). A novel mechanism for regulating clonal propagation of mouse ES cells. Genes Cells *9*, 471–477.

Ohbo, K., Yoshida, S., Ohmura, M., Ohneda, O., Ogawa, T., Tsuchiya, H., Kuwana, T., Kehler, J., Abe, K., Schöler, H.R., and Suda, T. (2003). Identification and characterization of stem cells in prepubertal spermatogenesis in mice small star, filled. Dev. Biol. *258*, 209–225.

Pérez-Victoria, F.J., Mardones, G.A., and Bonifacino, J.S. (2008). Requirement of the human GARP complex for mannose 6-phosphate-receptor-dependent sorting of cathepsin D to lysosomes. Mol. Biol. Cell *19*, 2350–2362.

Pérez-Victoria, F.J., Schindler, C., Magadán, J.G., Mardones, G.A., Delevoye, C., Romao, M., Raposo, G., and Bonifacino, J.S. (2010). Ang2/fat-free is a conserved subunit of the Golgi-associated retrograde protein complex. Mol. Biol. Cell *21*, 3386–3395.

Pfister, S., Steiner, K.A., and Tam, P.P. (2007). Gene expression pattern and progression of embryogenesis in the immediate post-implantation period of mouse development. Gene Expr. Patterns *7*, 558–573.

Radice, G., Lee, J.J., and Costantini, F. (1991). H beta 58, an insertional mutation affecting early postimplantation development of the mouse embryo. Development *111*, 801–811.

Rossant, J., Gardner, R.L., and Alexandre, H.L. (1978). Investigation of the potency of cells from the postimplantation mouse embryo by blastocyst injection: a preliminary report. J. Embryol. Exp. Morphol. *48*, 239–247.

Schmitt-John, T., Drepper, C., Mussmann, A., Hahn, P., Kuhlmann, M., Thiel, C., Hafner, M., Lengeling, A., Heimann, P., Jones, J.M., et al. (2005). Mutation of Vps54 causes motor neuron disease and defective spermiogenesis in the wobbler mouse. Nat. Genet. *37*, 1213–1215.

Schwarz, D.G., Griffin, C.T., Schneider, E.A., Yee, D., and Magnuson, T. (2002). Genetic analysis of sorting nexins 1 and 2 reveals a redundant and essential function in mice. Mol. Biol. Cell *13*, 3588–3600.

Seto, E.S., Bellen, H.J., and Lloyd, T.E. (2002). When cell biology meets development: endocytic regulation of signaling pathways. Genes Dev. *16*, 1314–1336.

Shaner, N.C., Steinbach, P.A., and Tsien, R.Y. (2005). A guide to choosing fluorescent proteins. Nat. Methods *2*, 905–909.

Silver, L.M. (1993). The peculiar journey of a selfish chromosome: mouse t haplotypes and meiotic drive. Trends Genet. *9*, 250–254.

Silver, L.M., and Artzt, K. (1981). Recombination suppression of mouse t-haplotypes due to chromatin mismatching. Nature *290*, 68–70.

Sorkin, A., and von Zastrow, M. (2009). Endocytosis and signalling: intertwining molecular networks. Nat. Rev. Mol. Cell Biol. *10*, 609–622.

Sugimoto, M., and Abe, K. (2007). X chromosome reactivation initiates in nascent primordial germ cells in mice. PLoS Genet. *3*, e116.

Sugimoto, M., Karashima, Y., Abe, K., Tan, S.S., and Takagi, N. (2003). Tetraploid embryos rescue the early defects of t^{w5}/t^{w5} mouse embryos. Genesis *37*, 162–171.

Tesar, P.J., Chenoweth, J.G., Brook, F.A., Davies, T.J., Evans, E.P., Mack, D.L., Gardner, R.L., and McKay, R.D. (2007). New cell lines from mouse epiblast share defining features with human embryonic stem cells. Nature *448*, 196–199.

Tomida, S., Mamiya, T., Sakamaki, H., Miura, M., Aosaki, T., Masuda, M., Niwa, M., Kameyama, T., Kobayashi, J., Iwaki, Y., et al. (2009). Usp46 is a quantitative trait gene regulating mouse immobile behavior in the tail suspension and forced swimming tests. Nat. Genet. *41*, 688–695.

Uehara, H., Abe, K., Park, C.H., Shin, H.S., Bennett, D., and Artzt, K. (1987). The molecular organization of the H-2K region of two t-haplotypes: implications for the evolution of genetic diversity. EMBO J. *6*, 83–90.

Vernet, C., Abe, K., and Artzt, K. (1998). Genetic mapping of 10 microsatellites in the t complex region of mouse chromosome 17. Mamm. Genome *9*, 472.

Yagi, T., Tokunaga, T., Furuta, Y., Nada, S., Yoshida, M., Tsukada, T., Saga, Y., Takeda, N., Ikawa, Y., and Aizawa, S. (1993). A novel ES cell line, TT2, with high germline-differentiating potency. Anal. Biochem. *214*, 70–76.